JARO 04: 130–138 (2003)
DOI: 10.1007/s10162-002-3015-9

JARO
Journal of the Association for Research in Otolaryngology

The Deaf Mouse Mutant *Jeff* (*Jf*) is a Single Gene Model of Otitis Media

Rachel E. Hardisty,[1] Alexandra Erven,[2] Karen Logan,[1] Susan Morse,[1] Sylvia Guionaud,[3] Sara Sancho–Oliver,[3] A. Jackie Hunter,[4] Steve D. M. Brown,[1] and Karen P. Steel[2]

[1]*MRC Mammalian Genetics Unit and UK Mouse Genome Centre, Harwell, OX11 0RD, UK*

[2]*MRC Institute of Hearing Research, University Park, Nottingham, NG7 2RD, UK*

[3]*Frimorpho Ltd., Chemin du Musee 12, C.P. 191, 1705 Fribourg, Switzerland*

[4]*GlaxoSmithKline, New Frontiers Science Park, Harlow, CM19 5AW, UK*

Received: 10 April 2002; Accepted: 5 August 2002; Online publication: 31 October 2002

ABSTRACT

Otitis media is the most common cause of hearing impairment in children and is primarily characterized by inflammation of the middle ear mucosa. Yet nothing is known of the underlying genetic pathways predisposing to otitis media in the human population. Increasingly, large-scale mouse mutagenesis programs have undertaken systematic and genome-wide efforts to recover large numbers of novel mutations affecting a diverse array of phenotypic areas involved with genetic disease including deafness. As part of the UK mutagenesis program, we have identified a novel deaf mouse mutant, *Jeff* (*Jf*). *Jeff* maps to the distal region of mouse chromosome 17 and presents with fluid and pus in the middle ear cavity. *Jeff* mutants are 21% smaller than wild-type littermates, have a mild craniofacial abnormality, and have elevated hearing thresholds. Middle ear epithelia of *Jeff* mice show evidence of a chronic proliferative otitis media. The *Jeff* mutant should prove valuable in elucidating the underlying genetic pathways predisposing to otitis media.

Keywords: otitis media, deafness, ENU mutagenesis, mouse genetics

INTRODUCTION

Otitis media, inflammation of the middle ear epithelial lining, remains the most common cause of hearing impairment in children (Davidson et al. 1989; Kubba et al. 2000). It is also the most common cause of surgery in children in the developed world. Two forms of chronic otitis media are generally known: chronic purulent otitis media (accompanied by tympanic membrane perforation) and chronic otitis media with effusion (Mawson 1974). Prolonged stimulation of the inflammatory response and poor mucociliary clearance can lead to the persistance of middle ear fluid giving rise to the clinical presentation of otitis media with effusion (OME) (Kubba et al. 2000). Risk factors include craniofacial abnormalities, impaired mucocilliary function, and the presence of an inflammatory stimulus, such as bacteria. Various sociological factors are also known to have a role, all of which relate to an increased propensity to infection (Kubba et al. 2000). There is evidence from studies of the human population that there is a significant genetic component predisposing to OME (Casselbrant et al. 1999), yet nothing is known about the underlying genetic pathways involved. In addition, there is still considerable debate over the etiology of OME and the underlying pathological mechanisms (Kubba et al. 2000).

Large-scale phenotype-driven ENU (*N*-ethyl-*N*-nitrosourea) mutagenesis programs in the mouse are a rich source of novel mutant phenotypes that can be used in systematic efforts for examining mammalian

REH and AE contributed equally to this study. SDMB and KPS are joint senior authors.

Correspondence to: Steve D. M. Brown • MRC Mammalian Genetics Unit • Harwell • OX11 ORD, UK. Telephone: 44 1235 824541; fax: 44 1235 824542; email: s.brown@har.mrc.ac.uk

gene function (Hrabe de Angelis et al. 2000; Nolan et al. 2000; Brown and Balling 2002). Moreover, they also can deliver powerful disease models that provide an effective route for elaborating the genetic pathways that may underlie human genetic disease (Nadeau et al. 2002). Recently, two large-scale dominant genome-wide ENU mutagenesis screens have been described. A variety of phenotype screens were employed covering a wide range of systems and around 1000 mutant phenotypes were identified (Hrabe de Angelis et al. 2000; Nolan et al. 2000). Many of the mutant phenotypes recovered potentially represent mutations at novel loci in the mammalian genome (Nolan et al. 2000).

Mouse models have played and continue to play an important role in studying the genetic causes of hearing impairment. A large catalog of mouse mutants that are deaf or demonstrate vestibular dysfunction is available. A number of these mutations have been cloned and have provided us with many profound insights into the critical proteins involved in the development and function of the auditory apparatus (Steel and Cros 2001; Brown and Steel 2002). Nevertheless, it is clear that we do not possess mouse mutants for all loci and pathways potentially involved in hearing impairment. In order to increase the breadth of mouse mutant models for hearing impairment, we have instituted a screen for deafness and vestibular phenotypes as part of the UK mutagenesis program (Nolan et al. 2000). Mutant mice were assessed for deafness and vestibular function as part of the SHIRPA screening protocol. As part of this protocol, mice were screened for deafness by recording the Preyer reflex in response to high frequency sound. A calibrated clickbox that generates a brief 20 kHz soundburst at 90 dB SPL was used in the UK ENU mutagenesis screen (Nolan et al. 2000). In order to detect a vestibular defect, a battery of specific balance tests was employed (Hardisty et al. 1999), including the contact righting test, the reaching response, and the negative geotaxis tests.

We have identified from the deafness screen in the UK mutagenesis program a novel hearing-impaired mutant, *Jeff*. Examination of the *Jeff* mutant showed that it had a chronic proliferative otitis media. The discovery and characterization of the *Jeff* mutant provides a new and important model for dissecting the underlying genetic causes of otitis media in the human population.

METHODS

Genetic mapping

We generated backcross progeny for mapping using the speed backcross approach already described (Isaacs et al. 2000). Briefly, backcross progeny are derived using *Jf/*+ sperm to fertilize C3H eggs. We phenotyped backcross progeny for deafness using a calibrated clickbox (20 kHz, 90 dB SPL, from the MRC Institute of Hearing Research, Nottingham, UK). Thirty DNAs were pooled from affected individuals and then genome scanned. Once a region of linkage was identified, we confirmed the map position by genotyping and haplotype analysis of individual affected backcross progeny.

FACS analysis

Seven *Jf/*+ mutant mice and 7 +/+ mice were rederived into isolators. Blood (300 μL) was taken from the tails of these animals at 43–44 days of age and 121–127 days of age and placed into EDTA-treated tubes; flow assisted cell sorting (FACS) analysis was carried out to identify levels of lymphocytes, neutrophils, CD4, CD19, CD3, and monocytes. Analysis was carried out on a Becton Dickinson FACSORT (BD, Franklin Lakes, NJ) using Cellquest (BD Biosciences, CA) software.

Histology

Twenty-three *Jf/*+ and 22 +/+ left-half adult heads (121–127 days old) were sectioned to investigate the *Jeff* middle ear and inner ear phenotype. Heads were bisected and fixed in 10% neutral buffered formaldehyde. Specimens were then decalcified in 10% formic acid in a 10% solution of sodium citrate. After rinsing in water, the half heads were put into EDTA for 14 days. After dehydration through graded alcohols, specimens were embedded in paraffin wax. Ten micrometer sections were cut in a saggital orientation. Sections were stained using a standard hematoxylin and eosin procedure. Newborn heads (8 *Jf/*+ and 7 +/+) were processed in the same manner without the decalcification steps.

3D reconstruction

Serial sections from single *Jf/*+ newborn and adult mice as well as single newborn and adult +/+ mice were captured using Zeiss Axioplan software and aligned by eye. Areas on images were selected in Adobe Photoshop (Adobe Systems Inc., San Jose, CA) and reconstructed using SlicerDicer software (Visualogic Inc, Bellevue, WA).

Physiology and ultrastructure

Middle ears were examined in urethane-anesthetized mice by opening the caudal wall of the middle ear during surgery to place a recording electrode, as well

as by later dissection (20 *Jf*/+ and 16 +/+ aged 26–53 days, 6 *Jf*/+ and 5 +/+ aged 11–28 months). Computer-averaged cochlear nerve compound action potentials were measured in response to calibrated tone burst stimuli, delivered through a closed sound system at frequencies between 3 and 30 kHz and at varying intensities, to establish thresholds (6 *Jf*/+ and 5 +/+ aged 34–37 days, 7 *Jf*/+ and 5 +/+ aged 11–28 months) as previously described (Steel and Smith 1992). However, the recording electrode in these experiments was placed upon the bony wall of the cochlea near the round window niche instead of on the round window in both mutants and controls, because of the difficulty in clearing and visualizing the round window in the mutant ears. Following response recording, the middle ear was opened further, a small hole made in the bony wall of the basal turn cochlear duct, and a 150 mM KCl-filled micropipette electrode inserted into the scala media to measure the endocochlear potential (16 *Jf*/+ and 13 +/+). After physiological recording, middle ear ossicles were dissected out and examined (10 *Jf*/+ and 9 +/+). Inner ears were cleared using standard techniques and examined for gross structural defects (4 *Jf*/+ and 5 +/+), and the surface of the organ of Corti and middle ear were examined by scanning electron microscopy (13 *Jf*/+ and 11 +/+) using standard techniques (Self et al. 1998).

Immunohistochemistry

Specimens (5 +/+ and 6 *Jf*/+) were treated as described above in the Histology subsection. Sections were deparaffinized for 15 minutes in xylene and put through two changes of 100% ethanol. Sections were then immersed in 0.3% hydrogen peroxide in methanol for 30 minutes. After washing in phosphate-buffered saline (PBS), sections were placed in a 0.2% solution of triton-X in PBS for 30 minutes. Sections were washed in PBS and blocked in 5% milk powder in PBS for 5 minutes. Antibodies raised to IL-1β, IL-8, and TNFα (Santa Cruz Biotechnology) were applied to the slides in a 1.5% solution of milk powder at a concentration of 10 μg/mL. Slides were left overnight at 4°C in a hydrated chamber. Slides were washed in PBS, and biotinylated horse antigoat secondary antibody (Vector Laboratories, Burlingame, CA) was applied in PBS for 30 minutes. Slides were washed again in PBS and the Avidin-Biotin complex (Vector Laboratories) was applied for 30 minutes. After further washing in PBS, slides were DAB stained until brown cells were apparent. The reaction was quenched in PBS and sections were counterstained with hematoxylin (blue coloration). Slides were mounted with aquamount (BDH Laboratory Supplies, UK), coverslipped, and photographed using a Zeiss Axioplan 2.

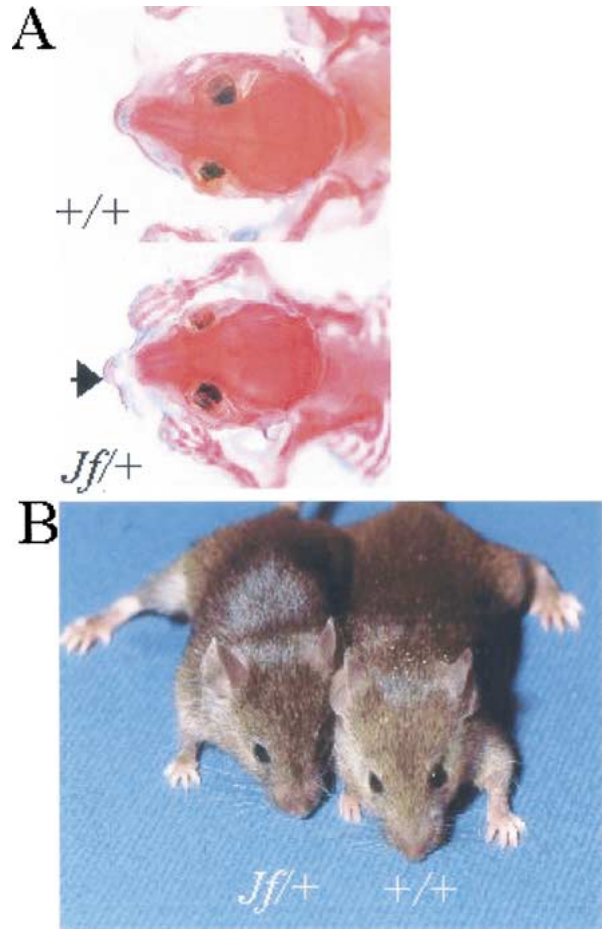

FIG. 1. The *Jeff* mouse mutant. **A**. Skeletal preparations of a *Jf*/+ and a control mouse. Shortened snout in adult *Jf*/+ mice is indicated by the arrow. **B**. Photograph of a *Jf*/+ mouse with its wild-type sibling indicating the smaller size of the mutant.

RESULTS

We identified the *Jeff* founder mutant mouse as it showed an absent Preyer response to a clickbox test indicating that it was deaf. Inheritance testing demonstrated that the *Jeff* deafness phenotype was fully penetrant from about 4 weeks of age, and transmission of the *Jeff* allele did not differ significantly from the expected 1:1 ratio ($X^2 = 0.19$, $df = 1$, $p > 0.1$). We found that all affected *Jf*/+ mice also demonstrated a shortened snout and occipital region compared with wild-type mice, indicating a mild craniofacial abnormality, but no other skeletal defects were evident (Fig. 1A). There was no significant variation of these features in the *Jeff* mice. We compared weights of adult *Jf*/+ mice to wild-type littermates and found *Jf*/+ mice to be 21% smaller (mean weight at 28 days: *Jf*/+, 17.0 ± 0.88 g; wild-type, 21.6 ± 0.32 g; one-way ANOVA, $F = 35.08$, $n = 51$, $p < 0.001$; see also Fig. 1B).

The gross structures of the middle ear ossicles and the inner ear were normal in *Jf*/+ mice, and scanning

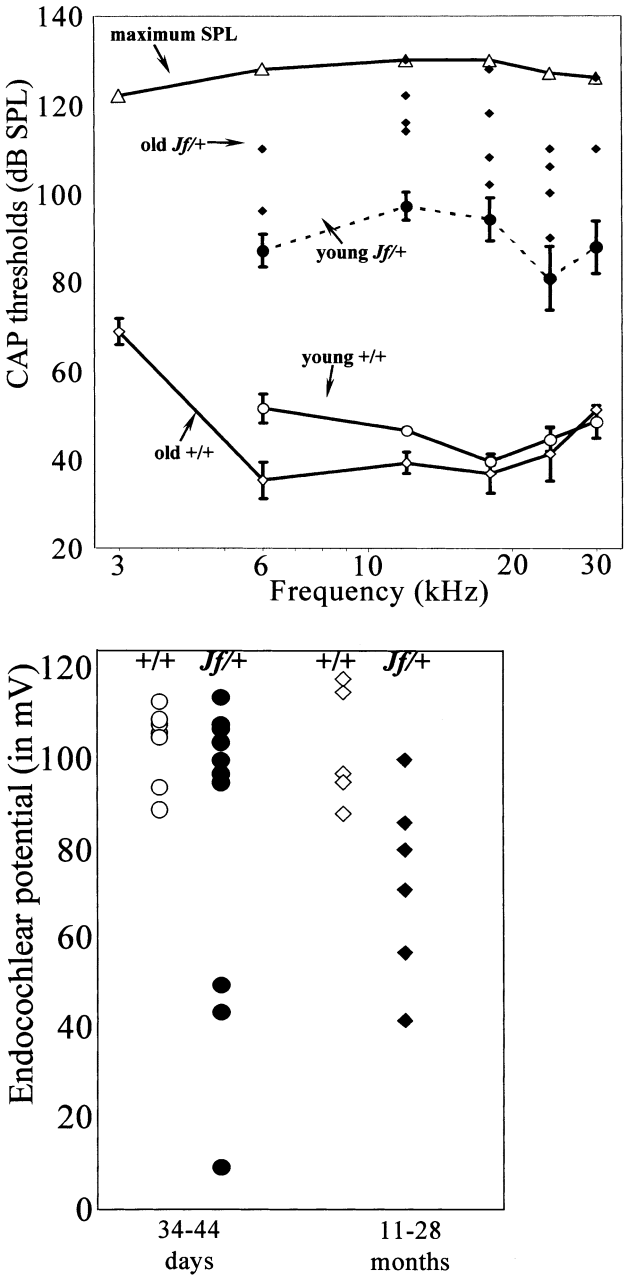

FIG. 2. Physiology of the *Jeff* mouse mutant. **Top**. Thresholds for detection of a cochlear nerve compound action potential. Young mice were aged 34–37 days old, and old mice were 11–18 months old. Two mutants aged 28 months showed no responses up to the peak output of the sound system (indicated by open triangles), and only a few responses to high-intensity stimuli were detected among the remaining old group of mutants aged 11–18 months, indicated by black diamonds. Remaining lines represent mean ± SEM. **Bottom**. Endocochlear potentials are plotted, showing abnormally low measurements in several of the mutants in both young and old age groups.

electron microscopy (SEM) of the organ of Corti showed no evidence of significant hair cell degeneration up to and including 18 months old (data not shown). Further investigation of the middle ear, however, showed *Jf*/+ mice had pus and fluid in the middle ear (ME) cavity. There were no obvious perforations of the tympanic membrane observed by gross inspection under a dissecting microscope, indicating that the *Jeff* mutant is a model of chronic otitis media with effusion. This was associated with raised thresholds for a cochlear nerve response (Fig. 2 top) in comparison with littermate controls, in which middle ear inflammation was never seen. In older mutants, thresholds were considerably raised, beyond the level that might be expected from a purely conductive impairment (Fig. 2 top). We measured the endocochlear potential, a resting potential of the fluid that bathes the upper surface of hair cells and which is generated by the stria vascularis of the cochlear duct. Several of the mutants showed abnormally low endocochlear potentials (Fig. 2 bottom), suggesting that impaired strial function might account for the sensorineural component of the hearing loss, although there were no obvious lateral wall defects observed in sections of *Jf*/+ cochleas (not shown). There have been many case reports of a sensorineural component to the hearing loss in humans with middle ear disease (Paperella 1991). Recent work implicates the lateral wall fibrocytes in cochlear pathology after experimental otitis media (Ichimiya et al. 2000) consistent with the reduced endocochlear potentials that we report.

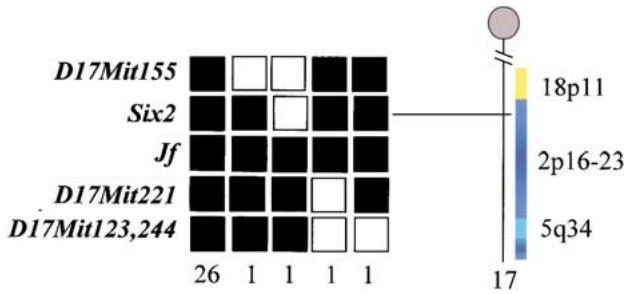

FIG. 3. Genetic mapping of the *Jeff* mutant. Speed backcrosses were utilized for the mapping of *Jeff*. *Jf*/+ sperm was used to fertilize C3H eggs, backcross progeny were phenotyped, and tail DNA from unaffected and affected individuals was prepared for genotyping (see Methods). Haplotypes of markers in the vicinity of *Jeff* are shown (filled boxes = BALB/c/C3H hybrids and *Jeff* mutants; open boxes = C3H homozygotes and wild-type mice at the *Jeff* locus). Marker and gene order is established by minimizing recombinants.Homology relationships to the human genome for distal mouse chromosome 17 are also shown. The gene *Six2*, which in human maps to 2p15–16 and lies within the conserved segment between mouse chromosome 17 and human 2p16–23, maps 1.96 ± 1.94 cM proximal to *Jeff*, indicating that the homolog of *Jeff* may map to human 2p. However, a single gene *DUSP*1 (mouse: *Ptpn*16), mapping to human 5q34, lies distal of *six*2 and disrupts this conserved segment.

We undertook the genetic mapping of the *Jeff* mutant using a speed backcross approach (Nolan et al. 2000), pooling of affected backcross progeny DNAs, and fluorescent genotyping with a panel of 100 microsatellite markers (Isaacs et al. 2000). Initial linkage to chromosome 17 was indicated and con-

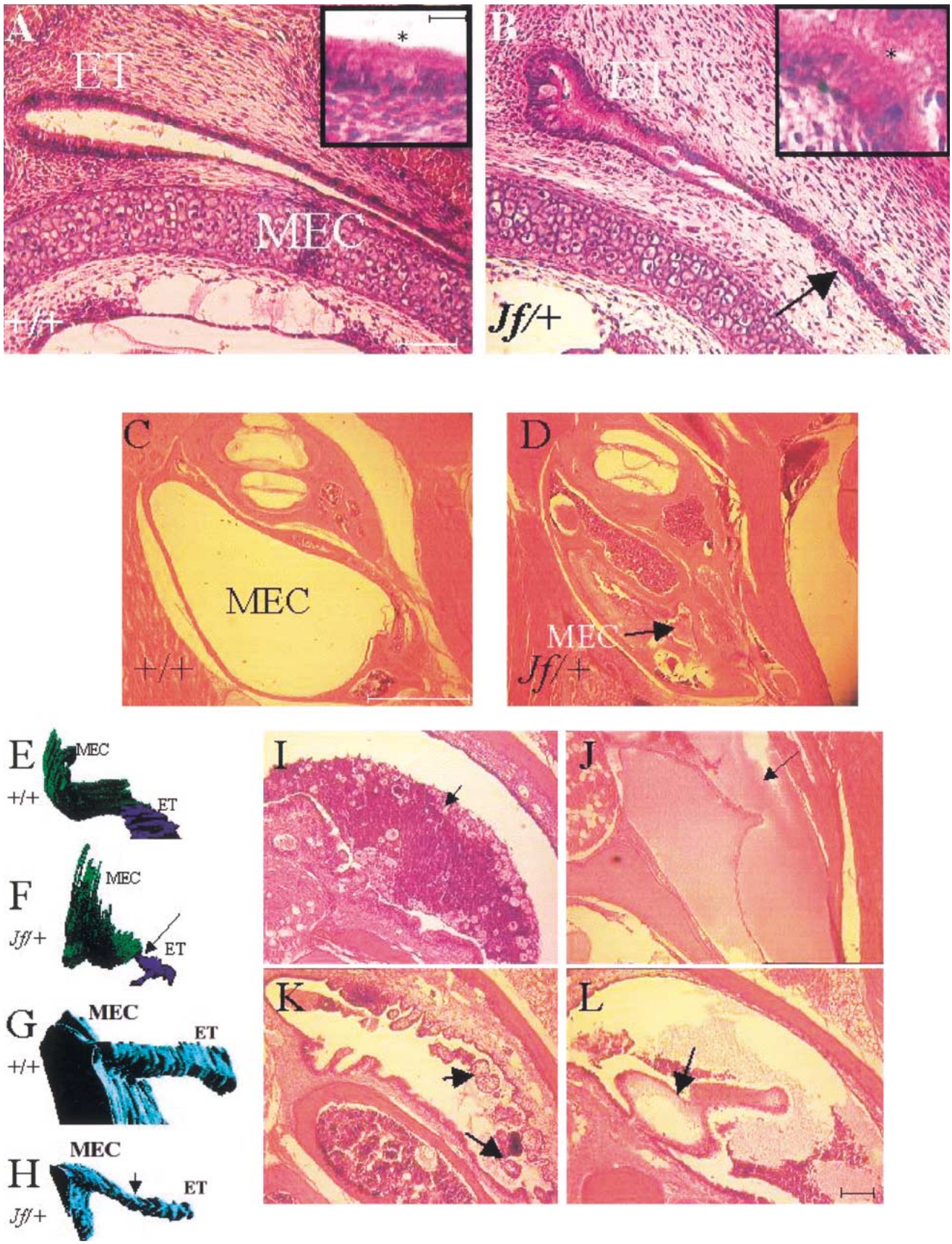
A
ET
MEC
+/+
B
Jf/+
C
MEC
+/+
D
MEC
Jf/+
E
MEC
+/+
ET
F
MEC
Jf/+
ET
G
MEC
ET
+/+
H
MEC
ET
Jf/+
I
J
K
L

FIG. 4. Structure and histopathology of the Eustachian tube and middle ear cavity in wild-type mice and +/*Jf* mice. **A,B**. Parasaggital sections through the newborn Eustachian tube joining the middle ear cavity. Inserts show epithelium (asterisks) at increased magnification. Arrow indicates collapsed middle ear cavity (MEC). Scale bar = 100 μm; inserts = 10 μm. **C,D**. Comparison of middle ear cavity size in wild-type and adult *Jf*/+ mice (*Jf*/+ = 121 days old, +/+ = 127 days old). Scale bar = 1 mm. **E,F**. 3D reconstructions of the Eustachian tube (ET) and middle ear cavity (MEC) in newborn wild-type and *Jf*/+ mice. The *Jf*/+ Eustachian tube is narrowed at the orifice of the middle ear cavity (arrow). **G,H**. 3D reconstructions of the Eustachian tube and part of the middle ear cavity in wild-type and *Jf*/+ mice. The bend in the *Jf*/+ Eustachian tube is indicated (arrow). (Mice were siblings and both aged 50 days). **I–L**. Histopathology of the middle ear cavity demonstrating middle ear glue (I and J, arrows) and polypoid exophytic growths that project into the tympanic cavity (K. and L, arrows). Scale bar = 100 μm.

firmed by genotyping of individual affected DNAs (Fig. 3). The *Jeff* mutation lies between the gene *Six*2 and the microsatellite marker *D17Mit221* on distal chromosome 17. These markers are 6.67 ± 4.55 cM apart. No other deaf mouse phenotype has been reported to map at this location. The distal end of mouse chromosome 17 encompasses a large conserved segment of homology with human chromosome 2 (2pl6–2p23) that includes *Six*2, suggesting that the human homolog of *Jeff* maps to this region. However, *Jeff* maps to the distal end of this conserved segment (see Fig. 3), and we have not shown that any other genes from human 2p map distal of *Jeff*. Therefore, we cannot rule out the possibility that the *Jeff* homolog maps to a different human chromosome region.

We carried out a detailed analysis of the structure of the ME cavity in newborn *Jf*/+ mice. *Jf*/+ mice were easily recognized at this age because of small body size and a blunt nose (see above). The lumen of the eustachian tube (ET) was smaller in *Jf*/+ newborn mice, though the scale of the reduction in size was variable (Fig. 4A,B,E,F). While some areas of the epithelial lining of the ET were intact, many regions were very disrupted, with cells sloughing off and accumulated cell debris in the lumen (see insert in Fig. 4A,B). In some newborn *Jf*/+ mice the ME cavity had apparently collapsed (Fig. 4B). We also examined the ME cavity and ET in adult *Jf*/+ mice. The ME cavity appeared to be reduced in size (Fig. 4C,D). Three-dimensional reconstruction demonstrated that the adult ET was

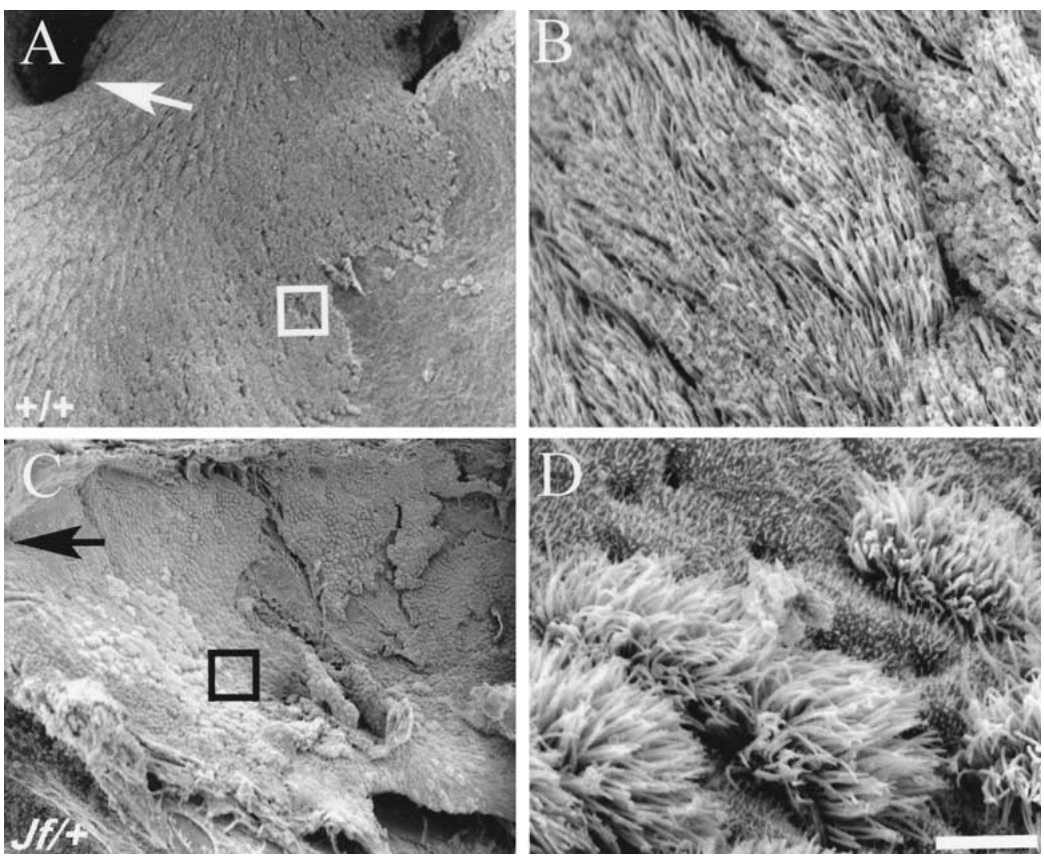

FIG. 5. Ultrastructure of middle ear epithelium in *Jeff* mice. **A–D**. Scanning electron micrographs showing the middle ear epithelium in control mice (**A,B**) and *Jf*/+ mutants (**C,D**) aged 11–18 months. In low magnification **A** and **C**, the start of the Eustachian tube is indicated by the arrow. The boxes indicate the area from which the higher magnifications (**B** and **D**) are taken. (**A**,**C**) Scale bar = 100 μm; (**B**,**D**) scale bar = 5μm.

narrower in adult *Jf/+* mice and was bent (Fig. 4G,H arrow). During surgery, the ME bony wall appeared thicker in mutants and the cavity was lined by a vascular membrane. Mutants aged 11 months and older also showed tympanic membrane retraction and excess calcification at scattered sites around the ME cavity, and the external ear was filled with cerumen.

Histolopathological examination demonstrated that *Jeff* showed a chronic proliferative otitis media. The mucosal inflammation was diffuse and of moderate severity. There were differing types of effusion: a dense granulocyte-rich effusion (Fig. 4I), a thin watery effusion (Fig. 4J) or a combination of both. The most striking lesions were papillary to polypoid exophytic growths that projected into the tympanic cavity (Fig. 4K,L arrows). These growths were covered with flat to cuboidal epithelium that appeared to be eroded in several areas. The projections were supported by moderate connective tissue stroma that was moderately to highly edematous and contained star-shaped fibroblasts. In the deeper layers of the submucosa, there were small accumulations of inflammatory cells and dilated lymphatics and blood vessels. There was evidence of inflammatory cell emigration through the epithelium. The polypoid projections were most likely due to fibroblast stimulation as a consequence of chronic inflammation. Polypoid projections were observed by SEM, which also revealed an intermixing of the ciliated cells with nonciliated cells instead of the distinct lawn of ciliated cells seen around the entrance of the eustachian tube in controls (Fig. 5A–D). The nonciliated cells appeared to have longer microvilli in mutants than in controls. These changes are similar to those described in otitis media following experimental eustachian tube obstruction (Kuijpers et al. 1984).

The *Jeff* mutant was initially discovered in a conventional facility. In order to determine if a pathogen-free environment would affect the development of otitis media in *Jeff* mutants, we rederived mice into both conventional and pathogen-free facilities. This experiment allowed us to investigate the development of otitis media in an environment devoid of the exogenous pathogens found in our conventional facility. Embryos obtained from IVF matings of *Jf/+* sperm to C3H/He eggs were reimplanted into foster mothers housed in conventional animal house space or in isolators. Surprisingly, we found that rederived mice in both environments developed deafness and affected mice had glue in their middle ears as observed in sections (data not shown). Of 14 mice transferred to isolators, 7 developed deafness, while 11 developed deafness out of 21 mice rederived into conventional facilities, consistent with Mendelian inheritance. We compared the immune status of *Jf/+* and wild-type mice raised in isolators. Age-matched *Jf/+* and *+/+* mice were compared at 43–44 days and 121–127 days for lymphocytes, neutrophils, monocytes, lymphocyte cell surface markers CD3, CD4, CD19, and MHC class II cell surface expression. At 43–44 days, the *Jf/+* mice born in isolators have a significantly higher number of neutrophils compared with control mice (mean value % neutrophils of stained cells for *Jf/+* mice = 18.37 ± 2.3; *+/+* = 12.84 ± 5.4, $p = 0.027$). Both *Jf/+* and *+/+* mice show similar low levels of MHC class II cell surface expression (mean value % of stained lymphocytes for *Jf/+* mice = 0.30 ± 0.21; *+/+* = 0.27 ± 0.16) that may indicate an inflammatory response occurring in *Jf/+* mice in the absence of an antigenic stimulus.

The cytokines TNFα, IL-1β, and IL-8 have been identified in 77–91%, 67–97%, and 92–100%, respectively, of chronic middle ear effusions in humans (Maxwell et al. 1994; Johnson et al. 1997). Cytokines are produced by inflammatory cells and play a role in controlling the acute inflammatory response. Also cytokines may be secreted by a variety of cells present in the innate and adaptive immune system as a result of an inflammatory stimulus. Induced animal models of otitis media suggest that one inflammatory stimulus is bacterial endotoxin, which stimulates TNFα production leading to mucin production and mucous hyperplasia (Ball et al. 1997; DeMaria and Murwin 1997; Rose et al. 1997; Hunter et al. 1999). Immunohistochemistry was carried out on *Jf/+* and *+/+* middle ear cavities with polyclonal antibodies raised to the cytokines TNFα, IL-1β, and IL-8. *Jeff* middle ear effusions stained strongly positive for all three cytokines (brown coloration from the DAB staining, Fig. 6A–D) in contrast with wild-type mice where no labeling was observed (data not shown).

DISCUSSION

The *Jeff* mutation maps to chromosome 17 and identifies a novel genetic locus involved in predisposition to OME. The main phenotype observed in *Jeff* mice is a chronic proliferative otitis media. *Jeff* mice develop OME in pathogen-free conditions, suggesting that they demonstrate either a genetically predisposed hypersensitivity to any normal endogenous bacteria that may still be present, or they show a constitutive inflammatory response that does not require an infection as a trigger. There is considerable disturbance to the structure of the *Jeff* eustachian tube that may contribute to the development of otitis media.

Increased susceptibility (in some animal house environments) to the development of an otitis media has previously been described in three inbred strains: C3H/HeJ, CBA/J, and LP/J (Steel et al. 1987; McGinn et al. 1992; Mitchell et al. 1997). In C3H/HeJ, the

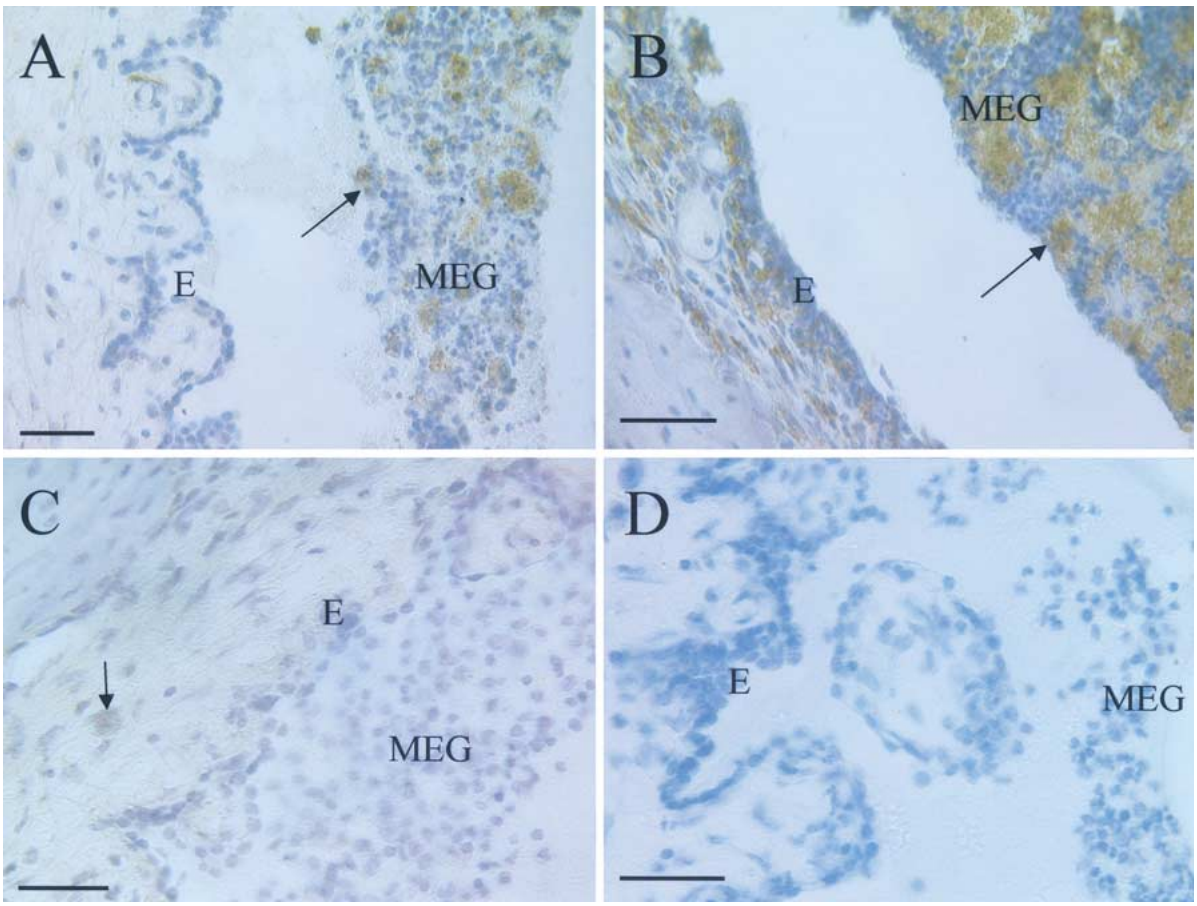

FIG. 6. Cytokine staining of middle ear effusions in *Jeff* mice. Immunohistochemistry was carried out on *Jf/+* and +/+ middle ear cavities with polyclonal antibodies raised to the cytokines TNFα, IL-1β, and IL-8 (all mice were 121 days old). Positively stained cells (indicated by arrows) were seen for all three cytokines: **A**. IL8, **B**. IL-1β, **C.** TNFα, **D**. Minus primary antibody control. Scale bars = 50 μM.

disease is not fully penetrant. Around 33% of mice develop an otitis media and age of onset varies widely from 2 to 18 months. Similarily, in CBA/J, by 180 days around 50% of mice have developed an otitis media. In LP/J, by 75 days 50% of mice had fluid in the middle ear cavity. This is in marked contrast to *Jeff* where the mutation is fully penetrant and all mice appear to be affected following weaning. In C3H/HeJ, nonresponsiveness to bacterial lipopolysaccharide (LPS) due to a gene defect on chromosome 4 may underlie the failure to clear middle ear disease (Mitchell et al. 1997), though this is not proven. The CBA/J mouse carries an X-linked defect in T helper cells that is responsible for B-lymphocyte maturation and may contribute to increased susceptibility to infection and the onset of otitis media (Goodman and Weigle 1979). Other genes may contribute to the susceptibility seen in CBA/J, C3H/HeJ, and LP/J.

p73-deficient mice also develop an otitis media, but this is part of a wider spectrum of infections including rhinitis and conjuctivitis (Yang et al. 2000). Similarly, mice with suppressed NF-KB function show chronic otitis media as one feature of a wide spectrum of phenotypes including defects in epidermal organogenesis (Schmidt–Ullrich et al. 2001). The chronic otitis media appears to be caused by *Staphylococcus aureus* infections resulting from macrophage dysfunction, though the susceptibility to otitis media may be compounded by impaired mucous gland function. A mouse model of Mucopolysaccharidosis type VII that lacks β-glucuronidase also develops otitis media, excess cerumen, and a mild craniofacial anomaly, among other diverse pathologic features associated with lysosomal storage disease (Berry et al. 1984).

We know nothing of the predisposing genetic factors to OME in the human population (Casselbrant et al. 1999) and, in addition, the etiology of OME and the underlying pathological mechanisms still remain relatively obscure. Other areas that clearly need to be addressed to further evaluate *Jeff* as a model for the study of otitis media are the function of the eustachian tube and its cilia, the status of the tubal muscles, and the identification of any pathogens that may contribute to the development of the disease. However, we have presented evidence for one major genetic locus predisposing to otitis media. The *Jeff* mutant will allow

us to describe the genetic basis for at least one major etiological factor in OME and to relate this to the developing pathology in both mouse and human.

ACKNOWLEDGMENTS

This work was funded by the Medical Research Council, GlaxoSmithKline, and the European Community (contract BMH4-CT97-2715). Thanks to Terry Hacker, Caroline Barker, and Adele Seymour for histology services; Peter Glenister, Claire Shearer, and Sian Clements for IVF; and Professor Mark Haggard and Mary Gannon for advice on human OME.

REFERENCES

BALL SS, PRAZMA J, DAIS CG, TRIANA RJ, PILLSBURY HC. Role of tumor necrosis factor and interleukin-1 in endotoxin-induced middle ear effusions. Ann. Otol. Rhinol. Laryngol. 106:633–639, 1997.

BERRY CL, VOGLER C, GALVIN NJ, BIRKENMEIER EH, SLY WS. Pathology of the ear in murine mucopolysaccharidosis type VII. Morphological correlates of hearing loss. Lab. Invest. 71:438–445, 1994.

BROWN SDM, BALLING R. Systematic approaches to mouse mutagenesis. Curr. Opin. Genet. Dev. 11:268–273, 2001.

BROWN SDM, STEEL KP. DFN genes. In: Creighton TE, (ed) Encyclopedia of Molecular Medicine. John Wiley & Sons, New York, 2002, pp 1035–1038

CASSELBRANT ML, MANDEL EM, FALL PA, ROCKETTE HE, KURS–LASKY CD, BLUESTONE CD, FERRELL RE. The heritability of otitis media. A twin and triplet study. JAMA 282:2125–2130, 1999.

DAVIDSON J, HYDE ML, ALBERTI PW. Epidemiologic parameters in childhood hearing loss: a review. Int. J. Pediatr. Otorhinolaryngol. 17:239–266, 1989.

DEMARIA TF, MURWIN DM. Tumor necrosis factor during experimental lipopolysaccharide-induced otitis media. Laryngoscope 107:369–372, 1997.

GOODMAN MG, WEIGLE WO. T cell regulation of polyclonal B cell responsiveness II. Evidence for a deficit in T cell function in mice with an X-linked B lymphocyte defect. J. Immunol. 123:2482–2487, 1979.

HARDISTY RE, MBURU P, BROWN SDM. mutagenesis and the search for deafness genes. Br. J. Audiol. 33:279–283, 1999.

HRABE DE ANGELIS M, FASWINKEL H, FUCHS H, RATHKOLB B, SOEARTO S, MARSCHALL S, HEFFNER S, PARGENT W, WUENSCH K, JUNG M, REIS T, RICHTER T, ALESSANDRINI F, JAKOB T, FUCHS E, KOLB H, KREMMER E, SCHAEBLE K, ROLLINSKI B, ROSCHER A, PETERS C, MEITINGER T, ASTROM T, STECKLER T, HOLSBOER F, KLOPSTOCK T, GEKELER F, SCHINDEWOLF C, JUNG T, AVRAHAM K, BEHRENDT H, RING J, ZIMMER K, SCHUGHART K, PFEFFER K, WOLF E, BALLING R. Genome-wide, large-scale production of mutant mice by ENU mutagenesis. Nat. Genet. 25:444–447, 2000.

HUNTER SE, SINGLA AK, PRAZMA J, JEWETT BS, RANDELL SH, PILLSBURY HC. Mucin production in the middle ear in response to lipopolysaccharides. Otolaryngol. Head Neck Surg. 120:884–888, 1999.

ICHIMIYA I, YOSHIDA K, HIRANO T, SUZUKI M, MOGI G. Significance of spiral ligament fibrocytes with cochlear inflammation. Int. J. Pediatr. Otorhinolaryngol. 56:45–51, 2000.

ISAACS AM, DAVIES KE, HUNTER AJ, NOLAN PM, VIZOR L, PETERS J, GALE DG, KELSELL DP, LATHAM ID, CHASE JM, FISHER EMC, BOUZYK M, POTTER A, MASIH M, WALSH FS, SIMS MA, DONCASTER KE, PARSONS CA, MARTIN J, BROWN SDM, RASTAN S, SPURR N, GRAY IC. Identification of two new *Pmp22* mouse mutants using large-scale mutagenesis and a novel rapid mapping strategy. Hum. Mol. Genet. 9:1865–1871, 2000.

JOHNSON IJ, BROOKS T, HUTTON DA, BIRCHALL JP, PEARSON JP. Compositional differences between bilateral middle ear effusions in OME: Evidence for a different aetiology. Laryngoscope 107:684–689, 1997.

KUBBA H, PEARSON JP, BIRCHALL JP. The aetiology of otitis media with effusion: a review. Clin. Otolaryngol. 25:181–194, 2000.

KUIJPERS W, VAN DER BEEK JMH, JAP PHK, TONNAER ELG. The structure of the middle ear epithelium of the rat and the effect of eustachian tube obstruction. Histochem. J. 16:807–818, 1984.

MAWSON SR. Diseases of the ear, 3rd ed. Edward Arnold Publishers Ltd., London, 1974, pp 284–285–285

MAXWELL KS, FITZGERALD JE, BURLESON JA, LEONARD G, CARPENTER DL, KREUTZER DL. Interleukin 8 expression in Otitis Media. Laryngoscope 104:989–995, 1994.

MCGINN MD, BEAN–KNUDSEN D, ERMEL R. Incidence of otitis media in CBA/J and CBA/CaJ mice. Hear. Res. 59:1–6, 1992.

MITCHELL CR, KEMPTON JB, SCOTT–TYLER B, TRUNE DR. Otitis media incidence and impact on the auditory brain stem response in lipopolysaccharide-nonresponsive C3H/HeJ mice. Otolaryngol. Head Neck Surg. 117:459–464, 1997.

NADEAU J, BALLING R, BARSH G, BEIER D, BROWN SDM, BUCAN M, CAMPER S, CARLSON G, COPELAND N, EPPING J, FLETCHER C, FRANKEL WN, GANTEN D, GOLDOWITZ D, GOODNOW C, GUENET JL, HICKS G, HRABE DE ANGELIS M, JACKSON I, JACON HJ, JENKINS N, JOHNSON D, JUSTICE M, KAY S, KINGSLEY D, LEHRAH H, MAGNUSON M, MEISLER M, POUSTKA A, RINCHIK E, ROSSANT J, RUSSELL LB, SCHIMENTI J, SHIROISHI T, SKARNES WC, SORIANO P, STANFORD W, TAKAHASHI JS, WURST W. Functional annotation of mouse genome sequences. Science 291:1251–1255, 2001.

NOLAN PM, PETERS J, STRIVENS M, ROGERS D, HAGAN J, SPURR N, GRAY L, VIZOR L, BROOKER D, WHITEHILL E, WASHBOURNE R, HOUGH T, GREENAWAY S, HEWITT M, LIU X, MCCORMACK S, PICKFORD K, SELLEY S, WELLS S, TYMOWSKA–LALANE Z, ROBY P, GLENISTER P, THORNTON C, THAUNG C, STEVENSON J-A, ARKELL R, MBURU P, HARDISTY R, KIERNAN A, ERVEN A, STEEL KP, VOGELING S, GUENET J, NICKOLS C, SADRI R, NAASE M, ISAACS AM, DAVIES K, BROWNE M, FISHER EMC, MARTIN J, RASTAN S, BROWN SDM, HUNTER AJ. A systematic, genome-wide, phenotype-driven mutagenesis programme for gene function studies in the mouse. Nat. Genet. 25:440–443, 2000.

PAPARELLA MM. Interactive inner ear/middle ear disease, including perilymphatic fistula. Acta Otolaryngol. Suppl. 485:36–45, 1991.

ROSE AS, PRAZMA J, RANDELL SH, BAGGETT HC, LANE AP, PILLSBURY HC. Nitric oxide mediates mucin secretion in endotoxin-induced otitis media with effusion. Otolaryngol. Head Neck Surg. 116:308–316, 1997.

SCHMIDT–ULLRICH R, AEBISCHER T, HULSKEN J, BIRCHMEIER W, KLEMM C, SCHEIDEREIT C. Requirement of NF-kB/Rel for the development of hair follicles and other epidermal appendices. Development 128:3843–3853, 2001.

SELF T, MAHONY M, FLEMING J, WALSH J, BROWN SDM, STEEL KP. Shaker-1 mutations reveal roles for myosin VIIA in both development and function of cochlear hair cells. Development 125:557–566, 1998.

STEEL KP, MOORJANI P, BOCK GR. Mixed conductive and sensorineural hearing loss in LP/J mice. Hear. Res. 28:227–236, 1987.

STEEL KP, SMITH RJH. Normal hearing in *splotch* (*Sp/+*), the mouse homologue of Waardenburg syndrome type 1. Nat. Genet. 2:75–79, 1992.

STEEL KP, CROS K. A genetic approach to understanding auditory function. Nat. Genet. 27:143–149, 2001.

YANG A, WALKER N, BRONSON R, KAGHAD M, OOSTERWEGEL M, BONNIN C, VAGNER C, BONNET H, DIKKES P, SHARPE A, MCKEON F, CAPUT D. p73-deficient mice have neurological, pheromonal and inflammatory defects but lack spontaneous tumours. Nature 404:99–103, 2000.